Zinc oxide nanoparticles prepared from diverse coordination compounds provide distinct mode of action and hemocompatibility

Hana Stepankova[1], Pavel Svec[1], Pavel Kopel[1], Marcin Swiatkowski[2], Rafal Kruszynski[2]
[1]Department of Chemistry and Biochemistry
Mendel University in Brno
Zemedelska 1, 613 00 Brno
CZECH REPUBLIC
[2]Institute of General and Ecological Chemistry
Lodz University of Technology
Zeromskiego 116, 90–924 Lodz
POLAND

hana.stepankova@mendelu.cz

Abstract: Eight different forms of zinc oxide nanoparticles (ZnO−NPs, labelled A−H) were synthetized. Basic toxicity testing has undergone for possible use in nanomedicine. The ZnO−NPs (A−H) stability in three different solutions was studied by scanning electron microscopy (SEM) and nanoparticle size. In addition, the ability to intercalate into DNA as well as the ability to cleave plasmid DNA were tested to verify the mechanism of toxicity. Subsequently, the hemocompatibility of nanoparticles was also examined.

Key Words: nanomedicine, nanoparticles, nanotoxicology, zinc oxide

INTRODUCTION

Due to its unique properties, inorganic and organic NPs are the focus of many years of research. NPs are a wide class of materials at nanoscale level with at least one dimension less than 100 nm (Laurent et al. 2008). Size reduction to nanoscale can tune its chemical, electrical, mechanical, morphological, optical and structural features and thus NPs can be able to interact with cell molecules and easily transfer into intracellular structures (Rasmussen et al. 2010, Pal et al. 2007). It allows applications in many fields, such as bionanotechnology, biosensors and nanomedicine. Based on the above, NPs can be sorted into different groups. Among others, these are ceramic NPs, carbon NPs, polymeric NPs, protein−based NPs and metal NPs (Laurent et al. 2008).

Metal−containing nanoparticles can be formed by ZnO, generally known for its useful antibacterial features. Also its photo−oxidizing and photocatalytic effects on organisms can be highly desirable (Sirelkhatim et al. 2015, Buzea et al. 2007). Although they have similar basic properties, the content of these NPs can provide different effects. In this project, eight different ZnO−NPs (termed A−H) were prepared and subject to various analyses aimed to evaluate their potential for nanomedical application.

MATERIAL AND METHODS

Chemicals

All chemicals of ACS purity were obtained from Sigma−Aldrich (St. Louis, MO, USA), unless stated otherwise.

ZnO−NPs synthesis and characterization

ZnO−NPs were synthesized using controlled thermal conversion of diverse coordination compounds (serving as precursors). For ZnO−A and ZnO−B, zinc formate was used for formation of the coordination compounds. For ZnO−C and ZnO−D, zinc acetate was used. Zinc propionate was used for synthesis of ZnO−E, zinc butyrate for synthesis of ZnO−F, zinc isobutyrate for ZnO−G

and zinc valerate for ZnO−H. Precursors for ZnO−A, C, E, F, G and H were added into corundum crucibles in air atmosphere and heated with heating rate of 1 °C/min. Precursors for ZnO−B and ZnO−D were heated with a heating rate of 10 °C/min. Other details of the synthesis as well as detailed characterization of the resulting NPs are not the subject of this manuscript as they have already been published elsewhere by Kruszynski and Swiatkowski (Kruszynski and Swiatkowski 2018, Swiatkowski and Kruszynski 2019).

Intercalation of ZnO−NPs into DNA

The stock dispersion of ZnO−NPs (A−H) with concentration of 1 mg/ml was prepared by dispersing NPs in deionized water and keeping samples in a sonication bath for 2 h. Subsequently, 1 µg of plasmid MP px459 was preincubated at 20 °C for 10 min with 6 µM ethidium bromide (EtBr) in PBS containing 10 mM NaCl (total volume 25 µl). After incubation, various concentrations of ZnNPs (A−H), (100; 50; 25; 12.5 µg/ml) were added (total volume 25 µl) and incubated for 10 min at 20 °C. Resulting EtBr fluorescence intensity was measured at 360 nm (excitation) and 600 nm (emission) using Tecan Infinite 200 PRO (Männedorf, Switzerland). As a control, 1 µg of plasmid MP px459 with 6 µM EtBr and ZnNPs−free PBS with 10 mM NaCl were used.

Plasmid cleaving assay

The stock dispersion of ZnO−NPs (A−H) was diluted to 500 µg/ml in 50 mM Tris−HCl buffer with 50 mM NaCl (pH 7.2). After that, plasmid MP px330 (50 ng/µl) was treated with the samples in final volume of 10 µl, followed by incubation at 37 °C for 1 h. Subsequently, loading buffer was added to the samples and mixtures were loaded in 1% agarose gel containing 55 ml of 40 mM Tris−acetate buffer, 1 mM EDTA and 2.5 µl of EtBr (10 mg/ml). Then the samples were subjected to electrophoresis in a horizontal gel apparatus for 90 min, at 75 V and RT. The final results of possible plasmid cleavage were displayed by using Azure c600 Azure Biosystems (Dublin, CA, USA). As control sample, solution of 50 mM Tris−HCl buffer with 50 mM NaCl with plasmid (50 ng/µl) with a final volume of 10 µl was used. 2−Log DNA Ladder was used to display the size of the DNA components.

Hemocompatibility

Fresh human red blood cells (RBCs) were used to determine the hemocompatibility of ZnO−NPs. 3 ml of blood was collected aseptically by antecubital venipuncture of healthy donor with signed informed consent. After the collection, RBCs were separated from plasma and leukocytes by centrifugation (5 min, 5,000 RPM, rotor ⌀ 16.8 cm, 20 °C). Collected suspension of RBCs was washed and centrifugated (5 min, 5,000 RPM, rotor ⌀ 16.8 cm, 4 °C) with 150 mM NaCl three to five times. Subsequently, concentrations 500; 250; 125; 62.5 µg/ml of ZnO−NPs (A−H) diluted in PBS (pH 7.4) were incubated with RBCs at 37 °C and 250 RPM for 1 h. As a negative control, RBCs with PBS were used. As a positive control, 0.1% Triton X−100 was used, causing complete lysis of RBCs. After incubation, the samples were centrifuged and the degree of hemolysis was determined by collecting supernatant, measuring the absorbance at 540 nm and calculating by the following equation: %hemolysis = [(At − Ac) /A100% − Ac)] × 100, where At is the absorbance of samples, Ac absorbance of negative control and A100% is the absorbance of positive control.

Physico−chemical characterization

To evaluate the stability of ZnO−NPs, samples were monitored in Ringer's solution (6.5 g NaCl, 0.42 g KCl, 0.25 g $CaCl_2$ and 0.2 g of sodium bicarbonate dissolved in 1 l of water) and medium RPMI 1640 containing 1 × Pen−Strep antibiotic (ATB) mixture (200 U/l penicillin, 0.2 mg/l streptomycin). The stock solutions (1 mg/ml) were dispersed in the mentioned solutions and sonicated in a sonication bath for 2 hours. Particle size was evaluated at different time points using particle size analyzer (Zetasizer Nano ZS90, Malvern instruments, Malvern, UK) and disposable cuvettes Zen 0040 (Brand GmbH, Wertheim, Germany), at a ratio of 1:200 of the stock sample with the solution (50 µl). During the experiment, the samples were kept at 37 °C. To monitor the morphological changes of ZnO−NPs in solution, they were dispersed in distilled water and imaged using a scanning electron microscope (SEM).

RESULTS AND DISCUSSION

The aim of the experiment was to determine the effect of ZnO−NPs by cytotoxic tests. First, the degree of intercalation capability of ZnO−NPs into DNA was detected (shown in Figure 1). EtBr has the ability bind to DNA by slipping between adjacent base pairs. However EtBr is not selective and has a low binding affinity (~10^5 M^{-1}), therefore substances with higher binding affinity can replace EtBr and reduce its fluorescence (Bugs and Cornelio 2001, Pastre et al. 2005). The experiment shows that as the concentration of ZnO−NPs decreases, the displacement rate also decreases. The highest percentage of intercalation was observed by using ZnO−A with concentration 1000 µg/ml (64% of intercalation), then ZnO−E (1000 µg/ml, 63%) and ZnO−H (1000 µg/ml, 62%). The lowest displacement was observed in ZnO−C (50.2%).

Figure 1 Intercalation of individual types and concentrations of ZnO−NPs into plasmid DNA (MP px459) after incubation with EtBr.

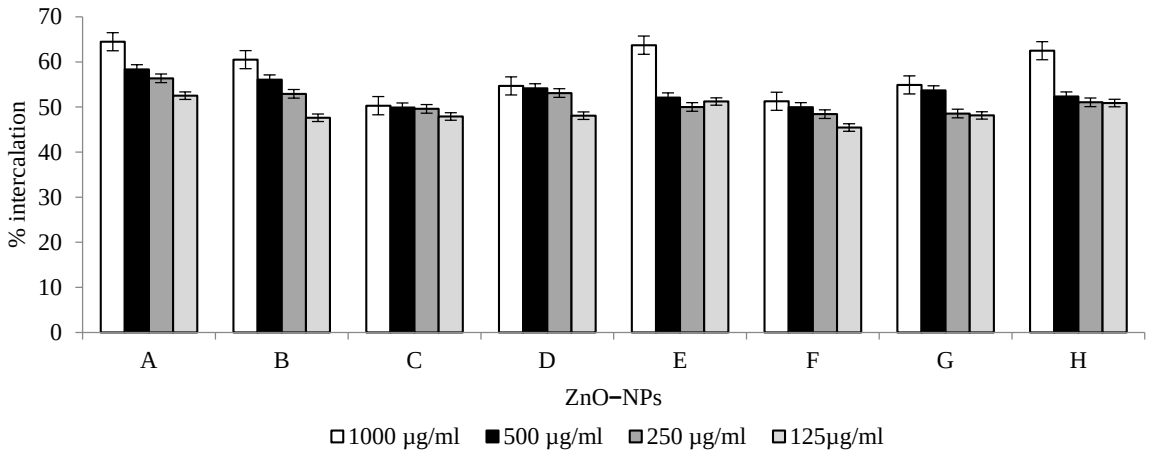

Figure 2 The ability to cleave plasmid DNA using different nanoparticles ZnO−NPs (A−H) with concentration 500 µg/ml. Cleavage results displayed on an agarose gel.

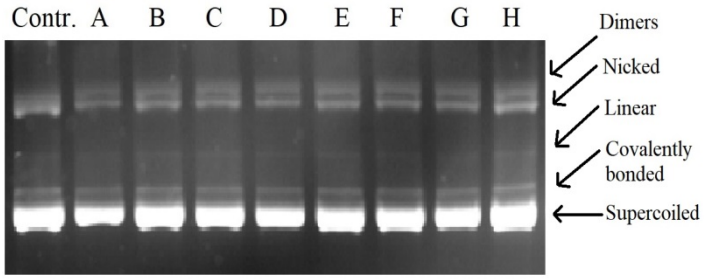

Figure 3 Quantification of the plasmid cleaving assay rate by plotting the different DNA forms in the graph with non−significant changes.

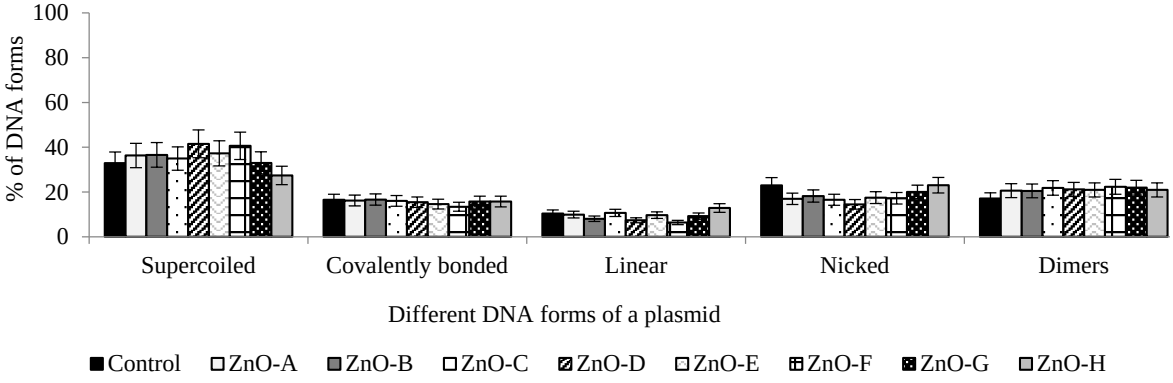

On the other hand, there were no significant changes in the plasmid structure during plasmid cleaving assay after adding ZnO−NPs (Figure 3). The first sample (Figure 2) displays a control without NPs where no plasmid cleavage can occur. Two clear and two thin bands show a common form of the used plasmid MP px459. Except for the highest bands with the presence of bifurcated structure next to the control, other plasmid−containing samples incubated with NPs show similar pattern of bands as the control sample. Therefore, although a slight cleaving of the DNA structure may occur by the effect of ZnO−NPs intercalation, most of the DNA remains intact.

Further, to determine the ability to lyse RBCs, NPs of various concentrations were tested for hemocompatibility. All samples showed a high rate of hemolysis at 0.5 mg/ml, with the highest level of hemolysis caused by ZnO−A (100%). Right behind were ZnO−G with 98% and ZnO−D (94% hemolysis). 90% was found in the ZnO−B sample. ZnO (C−F) caused hemolysis of ~80%. ZnO−H achieved the smallest percentage of hemolysis with 62%. Figure 4 shows the NPs with the highest hemolysis. However, the RBCs hemolysis was eliminated with lower concentrations of used ZnO−NPs.

Figure 4 Depicts the hemocompatibility results of ZnO−NPs. PBS represents negative control (100% hemocompatibility) and 0.1% Triton X−100 displays positive control (100% hemolysis). All displayed samples show at concentration 0.5mg/ml high hemolysis.

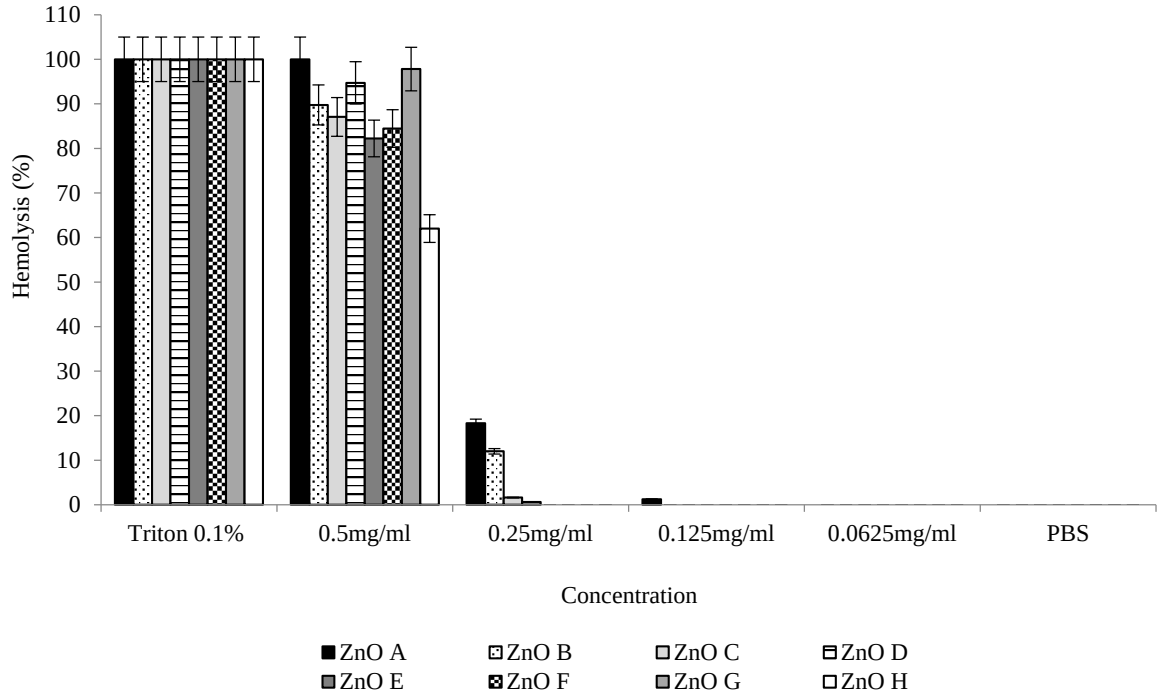

Another important parameter for nanomedical use is the NPs stability. For this purpose, ZnO−NPs were incubated in various solutions. One set of samples (A−H) was kept in Ringer's solution (isotonic solution simulating an environment of blood plasma), at 37 °C and was measured for three days to detect the formation of possible large aggregates. Second set of samples (A−H) was measured in the culture medium for several weeks to determine the length of stability in the stock solutions. The aim was to determine the presence of any aggregates of several µm. It was found that neither the Ringer's solution nor the medium caused any formation of clusters. This leads us to the prediction that once NPs will be introduced in real blood plasma, they will not clump together and may retain existing properties. However, further analyses are still necessary to evaluate the biocompatibility and stability of these particles.

To monitor the morphological changes of ZnO−NPs in solution, SEM micrographs were taken (Figure 5). Although no changes were observed for most of the tested ZnO−NPs for up to 72 h, slight dissolving of ZnO−A, ZnO−B and ZnO−F was observed after prolonged stay in water.

Figure 5 SEM micrographs of ZnO−NPs (B and G) in powder form and in Milli−Q after 24 h and 72 h. ZnO−B represents ZnO−NPs disolved in water after 72 h. ZnO−G represents ZnO−NPs stable in water for up to 72 h. The scale bar corresponds to 500 nm.

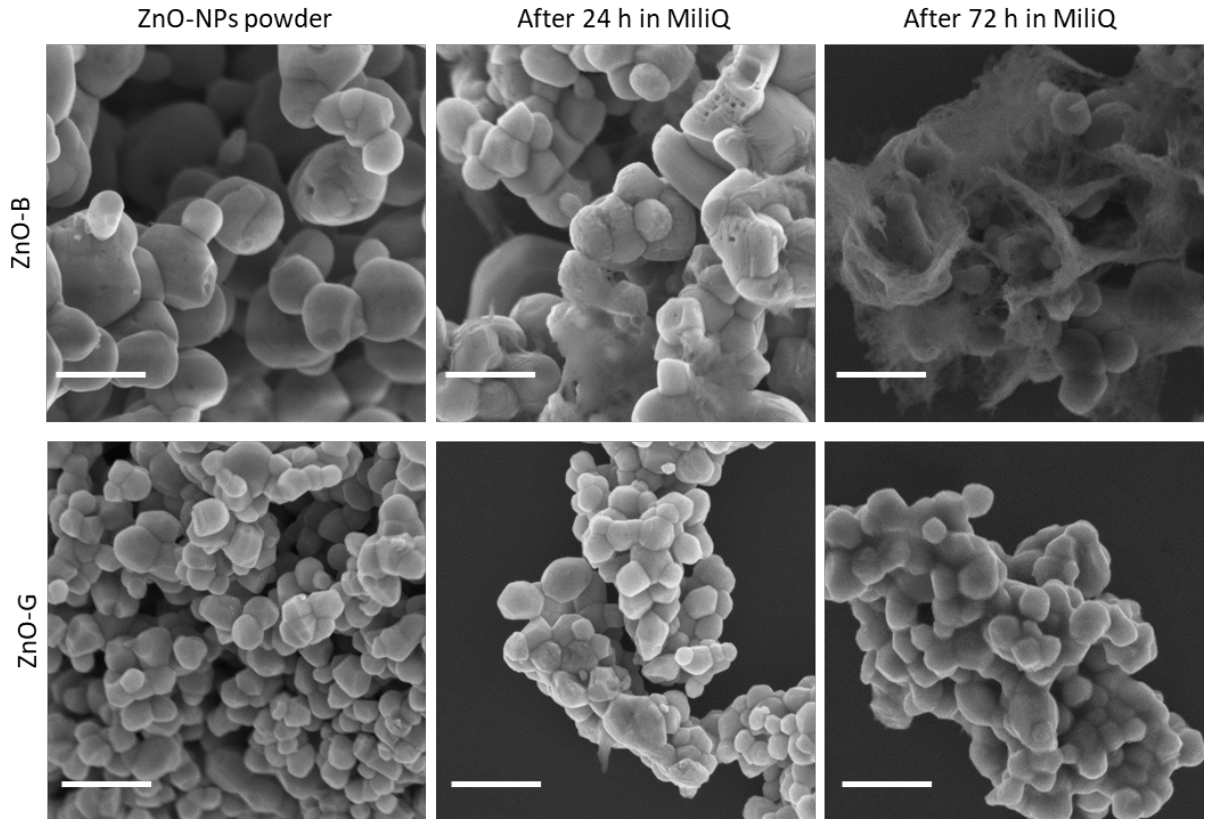

CONCLUSION

The general behaviour of ZnO−NPs and their mutual differences caused by using different precursors in the production process were studied by means of basic cytotoxicity tests. No nanoparticles showed significant ability to cleave plasmid DNA, while intercalation into DNA and hemolysis were demonstrated (ZnO A−H). ZnO−A, ZnO−B and ZnO−F showed higher solubility in water compared to others. ZnO−A appeared to be the most toxic, however, further testing is needed in the future for greater characterization.

ACKNOWLEDGEMENTS

The work was supported from ERDF "Multidisciplinary research to increase application potential of nanomaterials in agricultural practice" (No. CZ.02.1.01/0.0/0.0/16_025/0007314).

REFERENCES

Bugs, M.R., Cornelio, M.L. 2001. Analysis of the ethidium bromide bound to DNA by photoacoustic and FTIR spectroscopy. Photochemistry and Photobiology, 74(4): 512−20.

Buzea, C. et al. 2007. Nanomaterials and nanoparticles: sources and toxicity. Biointerphases, 2(4): 17−71.

Kruszynski, R., Swiatkowski, M. 2018. The structure of coordination precursors as an effective tool for governing of size and morphology of ZnS and ZnO nanoparticles. Journal of Saudi Chemical Society, 22(7): 816−825.

Laurent, S. et al. 2008. Magnetic iron oxide nanoparticles: synthesis, stabilization, vectorization, physicochemical characterizations, and biological applications. Chemical Reviews, 108(6): 2064−110.

Pal, S. et al. 2007. Does the antibacterial activity of silver nanoparticles depend on the shape of the nanoparticle? A study of the Gram−negative bacterium Escherichia coli. Applied and Environmental Microbiology, 73(6): 1712−20.

Pastre, D. et al. 2005. Study of the DNA/ethidium bromide interactions on mica surface by atomic force microscope: influence of the surface friction. Biopolymers, 77(1): 53−62.

Rasmussen, J.W. et al. 2010. Zinc oxide nanoparticles for selective destruction of tumor cells and potential for drug delivery applications. Expert Opinion on Drug Delivery, 7(9): 1063−77.

Sirelkhatim, A. et al. 2015. Review on Zinc Oxide Nanoparticles: Antibacterial Activity and Toxicity Mechanism. Nanomicro Letters, 7(3): 219−242.

Swiatkowski, M., Kruszynski, R. 2019. Structurally diverse coordination compounds of zinc as effective precursors of zinc oxide nanoparticles with various morphologies. Applied Organometallic Chemistry, 33(4): 1−18.